

# Soil Microbial Functional Succession Over One Year of Human Decomposition

Allison R. Mason<sup>1</sup>, Lois S. Taylor<sup>2</sup>, Naomi Gilbert<sup>1</sup>,  
Steven W. Wilhelm<sup>1</sup>, Jennifer M. DeBruyn<sup>1,2\*</sup>

<sup>1</sup>Department of Microbiology, University of Tennessee-Knoxville, 1311  
Cumberland Avenue, Knoxville, 37996.

<sup>2</sup>Department of Biosystems Engineering and Soil Science, University of  
Tennessee-Knoxville, 2506 E.J. Chapman Drive, Knoxville, 37996.

\*Corresponding author(s). E-mail(s): [jdebruyn@utk.edu](mailto:jdebruyn@utk.edu);

## Abstract

**Background** The succession of microbial communities during vertebrate decomposition has been observed in various settings, documenting changes in taxa as decomposition progresses. These studies have predominantly employed phylogenetic markers (*i.e.*, rRNA genes), describing community composition and structure, but ultimately are not informative of which members are active or metabolic pathways they might be expressing. This has left a foundational knowledge gap regarding the functional roles of microorganisms in vertebrate decomposition, which ultimately impact ecosystem functioning. Here we present the first known study investigating gene expression in soil impacted by human decomposition. Total RNA was extracted and metatranscriptomes obtained from soil samples collected over the course of one year from below three decomposing human bodies.

**Results** Microbial gene expression profiles shifted in response to decomposition: decomposition impacted soils were most different from controls (*i.e.* nearby soils unimpacted by decomposition) at day 86, and profiles remained altered even after

one year. Shifts in gene expression were partially explained by environmental and soil physiochemical variables, including internal body accumulated degree hours ( $p = 0.001$ ), as well as soil temperature ( $p = 0.045$ ), pH ( $p = 0.042$ ) and electrical conductivity ( $p = 0.037$ ). Differential expression analysis revealed that microbes in decomposition soils displayed increased expression of stress response genes (mean fold change 3.48), particularly heat shock proteins ( $p < 0.001$ ), whose expression increased between days 0 and 58 and remained elevated through day 376. Further, we identified genes whose expression was altered at certain time-points. This included increased expression of nitrogen cycling genes HAO (85x), norB (83x), and nosZ (19x) at day 86 when dissolved oxygen was ~85%, suggesting that microbial communities may be converting hydroxylamine to nitric oxide during reduced oxygen conditions.

**Conclusions** Our results show that human decomposition alters soil microbial gene expression profiles providing evidence of altered microbial metabolisms (*e.g.*, taurine metabolism, nitrogen cycling, and lipid metabolism) and reveal the potential of vertebrate decomposition to have both ephemeral and lasting effects on ecosystem processing in response to mortality events.

**Keywords:** Human Decomposition, Microbial Succession, Metatranscriptomics, Soil Microbial Ecology

## Introduction

Soil microbial communities are important drivers of ecosystem processes in terrestrial environments. Many soil microbes are decomposers that are involved in degradation of complex organic matter and drive nutrient cycling in terrestrial ecosystems. Environmental disturbances can impact the presence and/or activity of soil microorganisms that are involved in these cycles, ultimately affecting nutrient availability and the release of greenhouse gas emissions, such as CO<sub>2</sub> and N<sub>2</sub>O [1, 2]. Vertebrate death and subsequent carcass deposition in terrestrial ecosystems is one disturbance resulting in the deposition of large quantities of organic C and N [3–9], along with other elements (P, K, S, *etc*) [10], which collectively contribute to microbially-mediated

biogeochemical cycling. In addition to this, changes in pH, temperature, and fluctuations in soil oxygen provide abiotic filtering further impacting microbial metabolic strategies [6–8, 10, 11].

While C and N transformations have been documented during decomposition, the functional response of microbes and their roles in nutrient cycles remain unclear. Previous work from our lab [12, 13] and others [14–17] have conducted surveys of decomposition-impacted soil microbial communities through amplicon sequencing of marker genes (*i.e.*, 16S rRNA, 18S rRNA, ITS). This has allowed us to investigate changes in microbial biodiversity and composition in response to vertebrate decomposition, revealing patterns such as increases in the anaerobic taxa *Firmicutes* and *Bacteroidetes*. However, few studies have investigated soil biogeochemistry and microbial communities within the same study, which can further help to describe microbial ecology in human and animal decomposition systems. Taylor et al. (2024) [18] suggested that observed fungal community shifts were linked to soil dissolved oxygen, highlighting interactions between soil microbes and the surrounding environment. Additionally, Metcalf et al. (2016) [15] started to connect microbial changes to physiochemical data (*e.g.*, nitrate, pH) during controlled mouse decomposition experiments. While insightful for making potential connections between taxa and physiochemistry, these analyses cannot inform which taxa are active members of the community responsible for chemical transformations, which functional pathways/genes are expressed, and how these pathways are altered in response to decomposition.

Methods such as RNA sequencing (*i.e.*, metatranscriptomics) and metabolomics can be used to investigate microbial community functional succession in response to decomposition by measuring gene expression and metabolites, respectively. Where DNA-based methods are limited to explaining structural succession, analysis of microbial community gene expression (*i.e.*, mRNA) helps to determine which functional

139 pathways are altered in response to decomposition. This can inform how ecologi-  
 140 cal functions, including C and N cycling, are impacted by decomposition events in  
 141 terrestrial ecosystems. To date, only two studies have applied metatranscriptomic  
 142 approaches to assess mRNA in vertebrate decomposition samples [19, 20]: Burcham et  
 143 al. (2019) [19] examined gene expression of internal organ microbial communities dur-  
 144 ing mouse decomposition, while Ashe et al. (2021) [20] examined gene expression of  
 145 oral microbial communities during human decomposition. Both studies suggest that  
 146 the host microbial community functionality is altered during decomposition, includ-  
 147 ing differential expression of amino acid and carbohydrate metabolism in the heart  
 148 [19] and shifts in gene transcripts across different taxa [20]. We expect that soil  
 149 microbial community gene expression profiles are also altered; however, this has never  
 150 been examined to our knowledge. The decomposition-impacted soil metabolome was  
 151 assessed by DeBruyn et al. (2021) [21], showing changes in soil metabolites over time,  
 152 however it is unclear which microbes are responsible for these shifts. Additionally,  
 153 DeBruyn et al. (2021) [21] showed the soil metabolome was still altered compared to  
 154 starting conditions at the end of the 21-week study, suggesting long-term impacts of  
 155 decomposition on soil microbial functioning.

167 The purpose of this study was to investigate soil microbial gene expression during  
 168 a one-year period of human decomposition and address the following questions: (1)  
 169 which genes are differentially expressed in soils impacted by human decomposition?  
 170 (2) how does gene expression change over time in decomposition-impacted soils? (3)  
 171 do microbial gene expression profiles return to pre-decomposition conditions after one  
 172 year? The human body is comprised of carbon-rich organic molecules, many of which  
 173 are broken down during decomposition. We hypothesized that gene expression would  
 174 change over time as resources are used and transformed and soil chemical and phys-  
 175 ical conditions change as a result of tissue degradation [7, 8, 21]. For example, we  
 176 expected to observe changes in the expression of genes encoding enzymes involved in

nitrogen cycling, as increased nitrogen transformations have been previously described in decomposition soils [7]. Of the main macromolecules in the body (carbohydrates, proteins, lipids, and nucleic acids), we were particularly interested in lipid metabolism, as we expect lipids from the body to enter the soil during decomposition and previous studies showed an increase of lipolytic organisms in decomposition soils [22]. Finally, multiple studies have shown that soil chemistry [4, 7] and microbial community composition [12, 14] (via 16S rRNA gene amplicon sequencing) are still impacted after one year, therefore we did not expect soil expression profiles to return to pre-decomposition conditions.

To answer these questions, metatranscriptomes of soil samples collected at six key timepoints over one year of human decomposition were used to determine the active populations and expression of genes and pathways relevant to the enhanced biogeochemical cycling observed in decomposition hotspots. We compared gene expression between decomposition timepoints and control soils that were unexposed to decomposition products to identify functions or functional pathways of interest. This assessment of functional profiles within decomposition-impacted soils provided insight into the microbial response to vertebrate decomposition in terrestrial settings and biogeochemical cycling within these hotspots.

## Results

### Soil Physiochemistry

Soil chemistry was altered in response to human decomposition, with multiple parameters still impacted after one year [18]. Generally, soil pH decreased and remained low in decomposition soils of all but one individual. Soil electrical conductivity (EC) increased in response to decomposition, remaining elevated through approximately

day 58 before gradually decreasing throughout the remainder of the study (Supplementary Material 1). Respiration (evolved CO<sub>2</sub>) increased by an order of magnitude beginning at day 12, which corresponded to a reduction in soil dissolved oxygen (DO) to 29% - 48.9%. Ammonium concentrations increased 78-fold, reaching maximum concentrations between days 12 and 58. This was followed by decreased ammonium and increased nitrate concentrations at day 86, with nitrate concentrations reaching a maximum at day 168 (Supplementary Material 1).

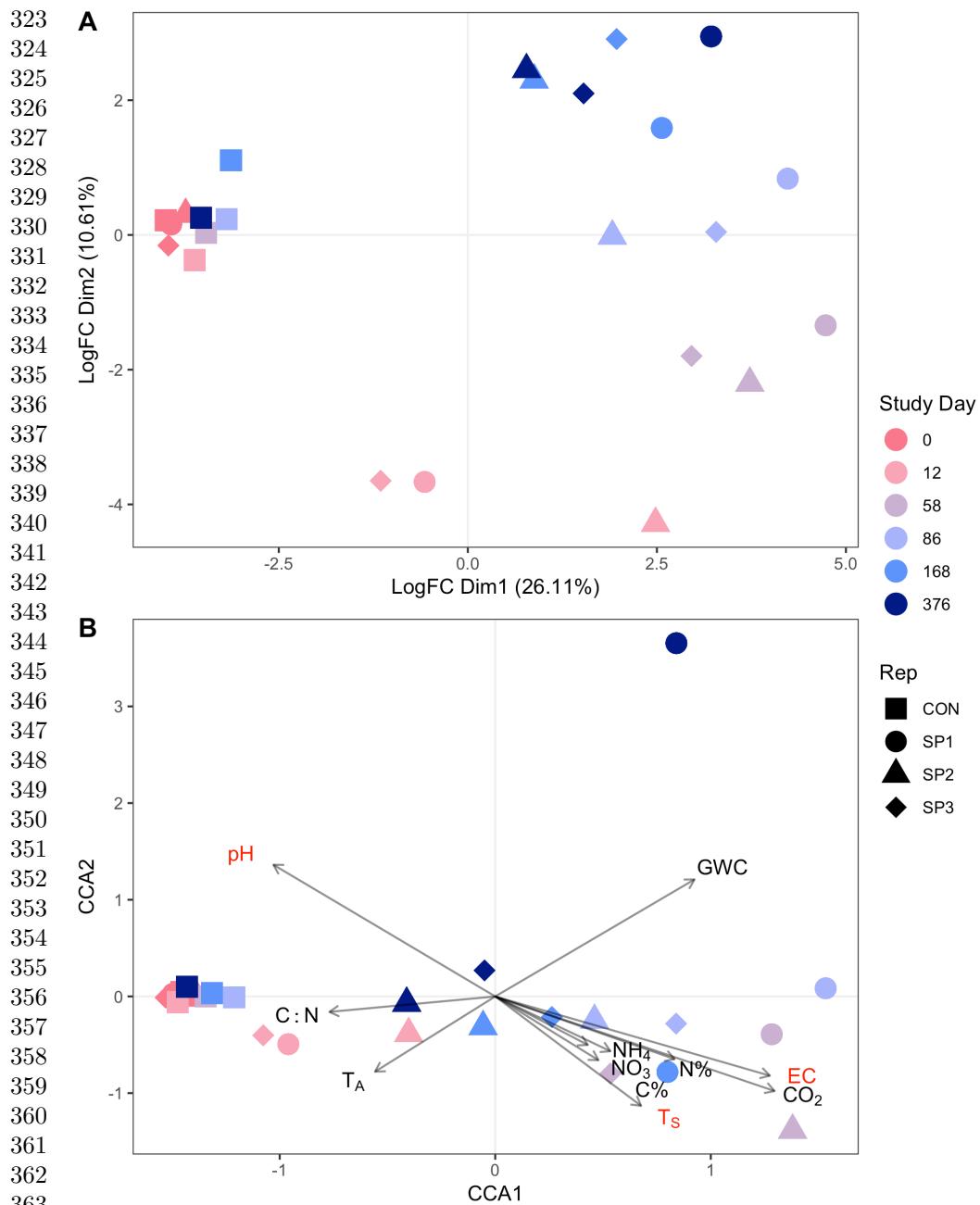
## Sequencing

Illumina sequencing of the 24 libraries yielded a total of 5,073,476,730 reads, or 2,536,738,365 paired reads, with a mean of 105,697,432 paired reads per sample. Removal of adapters and low-quality reads removed 4.7% of all reads, leaving 4,834,123,062 total reads. Filtering of ribosomal RNA further removed 7.3% of reads, leaving 4,479,804,360 reads for assembly. After co-assembly, a total of 6,257,674 proteins were identified by Prodigal. From this, 1,048,573 proteins were annotated by eggNOG-mapper (16.7%). Most of the annotated proteins were taxonomically annotated as bacteria (91.3%), followed by eukaryotes (7.6 %), and archaea (0.81 %). Of the 7.6% of eukaryotic proteins, 64.4% (4.9% of all proteins) were annotated as fungi. For this study, genes of interest included all bacterial, archaeal, and fungal proteins, therefore all non-fungal eukaryotic proteins (32,004) were removed prior to downstream analysis. The reference file of genes was then used to determine gene transcript counts in all samples using CLC genomic workbench. The percent of reads mapped to genes of interest ranged from 21% to 38%, with an average of 31% reads mapped. Gene counts were then combined in a single file and used for downstream analyses in R.

## Microbial gene expression in response to human decomposition

Gene expression profiles in decomposition-impacted soils shifted away from controls and day zero samples as decomposition progressed (Fig 1A). Expression was most different from controls on study days 58, 86, 168 (Supplementary Material 2), before shifting back toward control conditions on study day 376. After one year of decomposition, soil gene expression profiles had not returned to pre-decomposition conditions, as evidenced by their clustering away from controls and day zero samples in the MDS plot (Fig 1A).

**Figure 1: Microbial gene expression profiles are altered during human decomposition.** Multidimensional scaling (MDS) shows gene expression within soils changed as decomposition progressed (A). Additionally, canonical correspondence analysis (CCA) shows that environmental variables explained 64.3% of the variation in gene expression profiles (B). Variables in bold red type significantly ( $p < 0.05$ ) explained some of the variation in gene expression profiles as assessed by Permutational Analysis of Variance (PERMANOVA). In both panels soils from controls (CON) and the three donors (SP1, SP2, SP3) are denoted by symbol shape, while color represents study day. In B, soil physiochemical variable loadings are represented by arrows: Gravimetric water content (GWC), electrical conductivity (EC), pH (pH), respiration (evolved  $\text{CO}_2$   $\mu\text{mol gdw}^{-1}$ ), ammonium ( $\text{NH}_4$ ), and nitrate ( $\text{NO}_3$ ) concentrations ( $\text{mg gdw}^{-1}$ ), percent carbon (%C), percent nitrogen (%N), carbon:nitrogen ratio (C:N), ambient temperature ( $T_A$ ), and soil temperature ( $T_S$ ).



Some correlations were observed between gene expression shifts and soil physiochemical data at decomposition timepoints. Canonical correspondence analysis (CCA) was

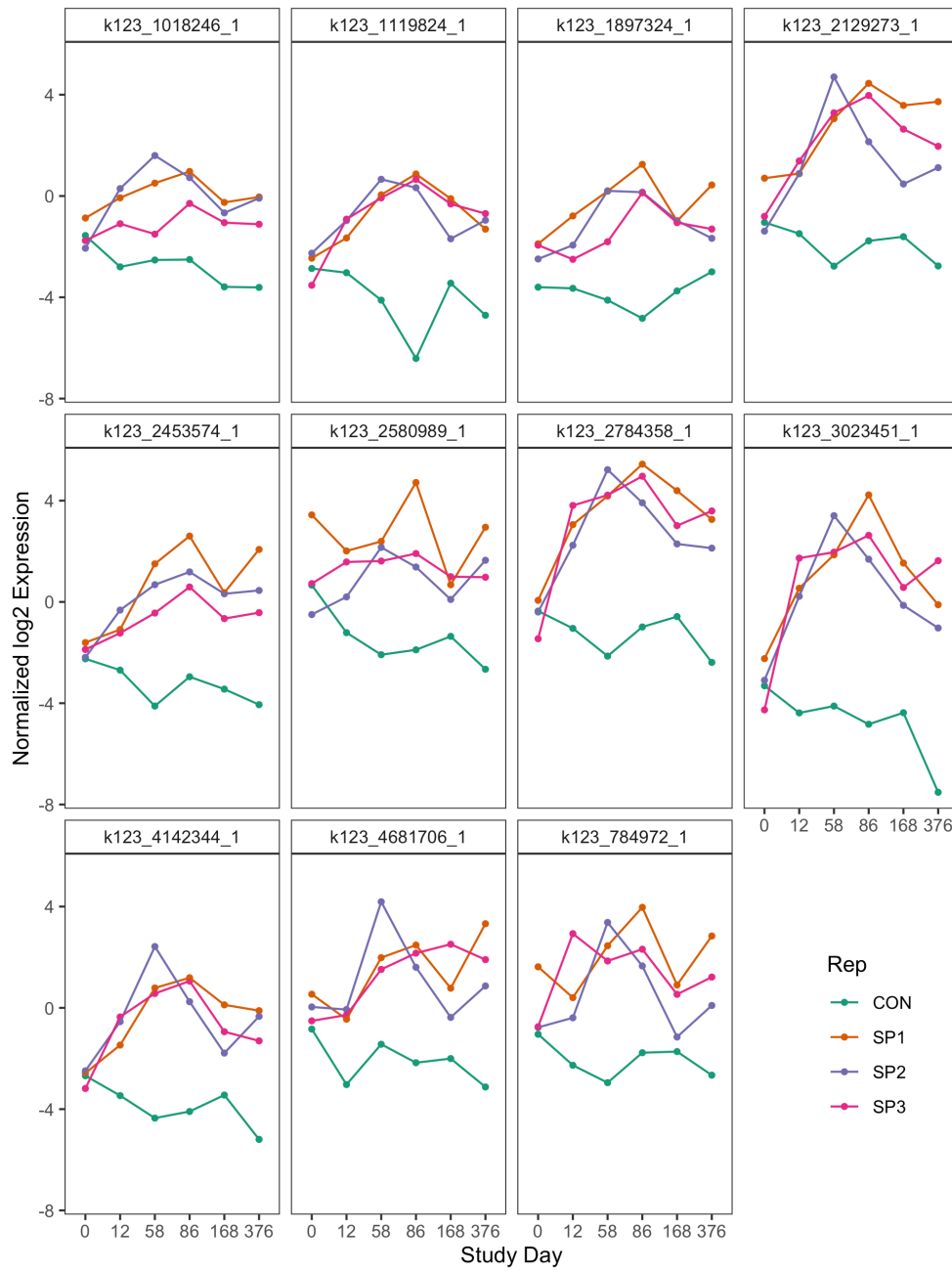


used to constrain gene expression data with soil physiochemical data (Fig 1B). CCA1 and CCA2 explained 36.2% and 20.9% of the variance in gene expression, respectively. Transcript profiles at day 12 were associated with an increase in soil carbon to nitrogen ratio (C:N). Gene expression profiles at days 58 to 86 were positively correlated with increased soil temperature, EC, and evolved CO<sub>2</sub>, while study day 168 was associated with elevated levels of soil NO<sub>3</sub>. Further, Permutational Analysis of Variance (PERMANOVA) revealed that internal accumulated degree hours (ADH), soil temperature, pH, and EC significantly explained some of the variation in gene expression profiles ( $p < 0.05$ ). No other soil chemical variables were significant at  $\alpha = 0.05$  (Supplementary Material 3).

Overall, decomposition changed soil gene expression profiles over the one-year study relative to control soils. Differential expression analysis between decomposition and control soils identified 7,047 down-regulated and 38,425 up-regulated genes. Gene transcripts that were associated with control soils comprised a wide variety of clusters of orthologous genes (COG) functional categories. Specifically, the top 20 genes whose expression was higher in control soils belonged to ten unique COG categories, including signal transduction mechanisms, transcription, and those of unknown function. In contrast, the top 20 genes whose expression was higher in decomposition soils only fell into four COG categories (Supplementary Material 4 A): 1) post-translational modification, protein turnover, and chaperones; 2) energy production and conversion; 3) cell motility; and 4) carbohydrate transport and metabolism. The most common COG category represented in decomposition soils (80%) were post-translational modification, protein turnover, and chaperones. Within this category, several heat shock stress response genes were identified, including SSA2, HSP82, and clpB (Supplementary Material 5). Further investigation into these genes shows their expression increased in response to decomposition, typically reaching maximum transcript levels around study days 58 and 86 (Fig 2). This corresponded to elevated soil temperatures below

decomposing bodies between study days 12-80, with soil temperatures increasing to approximately 43°C [18], and maximum soil EC measurements between days 12 and 58 (Supplementary Material 1).

**Figure 2: Normalized log2 expression of heat shock proteins identified by differential expression analysis comparing decomposition and control soils.** Each panel represents a single heat shock transcript, labeled with query ID. Symbol color denotes if the sample is a control (CON, green), or one of three individuals: SP1 (orange), SP2 (purple), or SP3 (pink).



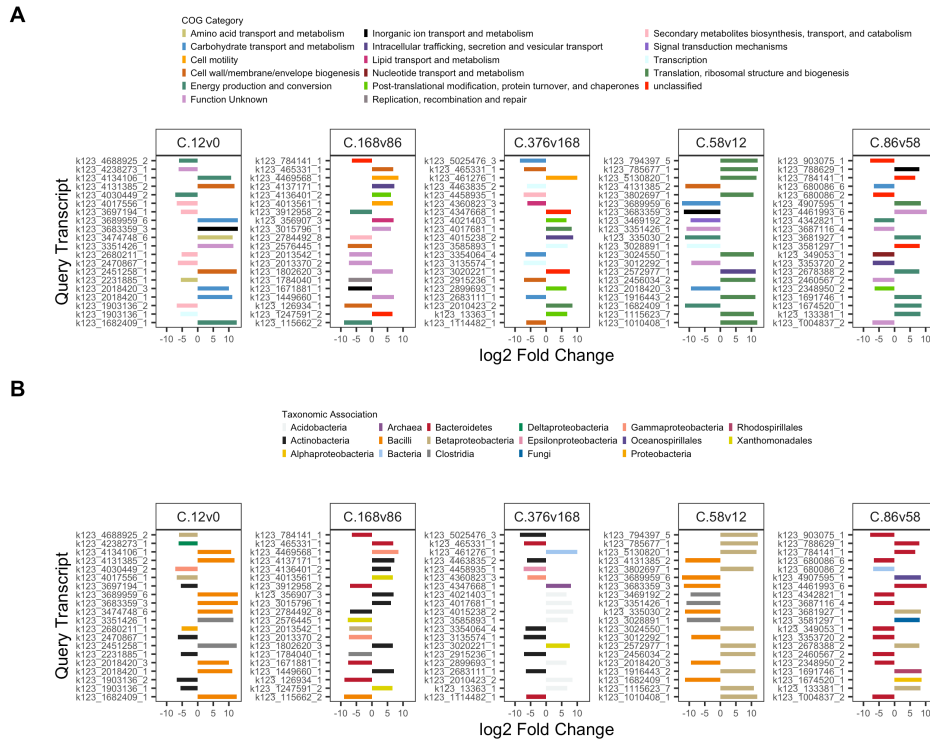
Taxonomy associated with top differentially expressed gene transcripts also differed between control and decomposition soils. The top 40 significantly differentially

expressed gene transcripts in decomposition soils were associated with Fungi, *Actinobacteria*, and *Xanthomonadales*, while gene transcripts in controls were associated with *Acidobacteria*, *Cyanobacteria*, *Proteobacteria* ( $\alpha$ ,  $\delta$ ,  $\gamma$ ), and Planctomycetes (Supplementary Material 4 B). The greatest number of differentially expressed genes relative to control samples was observed at day 86, where we saw 145,460 and 124,883 up- and down-regulated genes, respectively.

## Fate of decomposition products as evidenced in gene expression profiles over time

Differential expression analysis between respective sequential study days further revealed which genes were altered between decomposition timepoints. The top ten significantly up- and down-regulated genes, determined by the lowest p-values from differential expression analysis ( $< 0.05$ ), are reported in Supplementary Material 6 and Fig 3.

**Figure 3: Top twenty up- and down-regulated genes in decomposition soils comparing sequential study days (0, 12, 58, 86, 168, 376) colored by COG functional category (A) and taxonomic annotation (B).** Positive values denote increased expression compared to the preceding timepoint, while negative values denote a decrease.



Expression of genes annotated with the COG categories cell wall/membrane/envelope biogenesis, inorganic ion transport and metabolism, and carbohydrate transport and metabolism increased from day 0 to 12. In contrast, expression of secondary metabolite biosynthesis, transport, and catabolism genes decreased during this period (Fig 3A). Transcripts from *Bacilli* and *Clostridia* increased, while transcripts from *Actinobacteria* decreased between study days zero and 12 (Fig 3).

Between days 12 and 58, 90% of the topmost upregulated genes were associated with the COG translation, ribosomal structure and biogenesis and all were taxonomically associated with *Betaproteobacteria* (Fig 3A,B). Many of these genes were annotated as proteins within the *rpl* protein family, involved in ribosomal binding. Genes across multiple COG categories with taxonomic associations to *Bacilli* and *Clostridia* decreased

599 between study days 12 and 58, six of which were transcripts that previously increased  
600  
601 between days zero and 12 (Fig 3B, Supplementary Material 6).

602  
603 Multiple transcripts associated with the energy production and conversion COG, as  
604  
605 well as transcripts annotated with the COGs inorganic transport and metabolism,  
606  
607 and translation, ribosomal structure and biogenesis, increased between days 58 and  
608 86 (Fig 3A). Two of the upregulated energy and production and conservation tran-  
609  
610 scripts were associated with cytochrome c oxidase subunits in *Betaproteobacteria*,  
611  
612 while another was annotated as *hao*, encoding the enzyme hydroxylamine dehydroge-  
613  
614 nase which is involved in conversion of hydroxylamine to nitrite during nitrification  
615 (Supplementary Material 6). Further investigation into hydroxylamine dehydrogenase  
616  
617 showed a significant increase in *hao* transcripts at day 86 followed by subsequent  
618  
619 decreases at days 168 and 376 ( $F = 4.183$ ;  $p = 0.02$ ). This increase corresponded to  
620  
621 decreased soil ammonium levels and subsequent accumulation of nitrate (Supplemen-  
622  
623 tary Material 1). Half of the topmost downregulated genes between days 58 and 86  
624  
625 were not assigned to a COG (*i.e.*, unclassified) or were of unknown function.

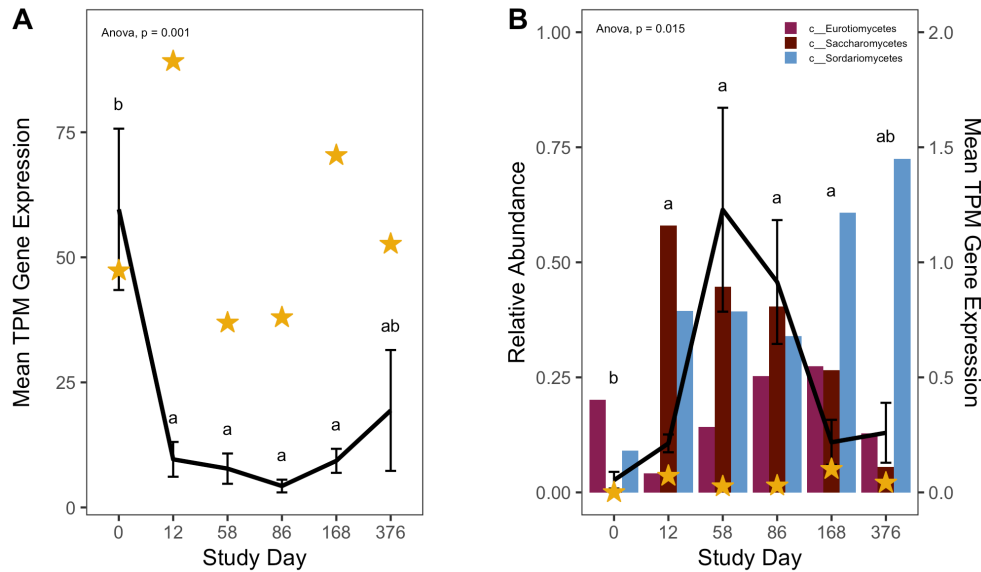
626 Differential expression comparing study days 86 with 168 and 168 with 376 iden-  
627  
628 tified genes across a variety of functional categories, with many unclassified in the  
629  
630 COG database or with unknown function (Fig 3A). Expression of carbohydrate trans-  
631  
632 port and metabolism genes associated with *Bacilli* decreased between day 168 and  
633  
634 376. Additionally, *Acidobacteria* transcripts increased in decomposition-impacted soils  
635  
636 between study day 168 and 376 (Fig 3B). These transcripts were not associated with  
637  
638 any single COG category, however.

## 639 **Carbon-dominant molecules**

640  
641 We expected to observe increased expression of lipid metabolizing genes during active  
642  
643 and advanced decomposition as microbes degraded lipids deposited in the soil [22].  
644

Therefore, we investigated changes in triacylglycerol lipase (enzyme commission number: 3.1.1.3) gene transcription in our soils. Generally, lipase transcripts decreased as decomposition progressed (HLM  $F = 6.564$ ,  $p < 0.001$ ), however we also observed a significant interaction between study day and taxonomic annotation ( $F = 8.786$ ;  $p < 0.001$ ). Specifically, lipase gene transcripts annotated as bacteria decreased with decomposition time ( $F = 10.392$ ;  $p = 0.001$ ), while fungal lipase transcripts increased, reaching a maximum at study day 58 ( $F = 4.509$ ;  $p = 0.015$ ) (Fig 4).

**Figure 4: Mean transcript abundance, in transcripts per million (TPM), of all bacterial (A) and fungal (B) triacylglycerol lipase (EC 3.1.1.3) genes over time.** Black lines (A, B) report mean and standard deviation of TPM from three individuals (black line), while gold stars denote mean TPM in control soils. P-values are the result of ANOVAs where average TPM and study day are the dependent and independent variables, respectively, while letters are the result of post-hoc Tukey tests between decomposition timepoints. In B, bars show the relative abundance of the fungal classes *Saccharomycetes*, *Sordariomycetes*, and *Eurotiomycetes*, reported in Taylor et al. (2024).

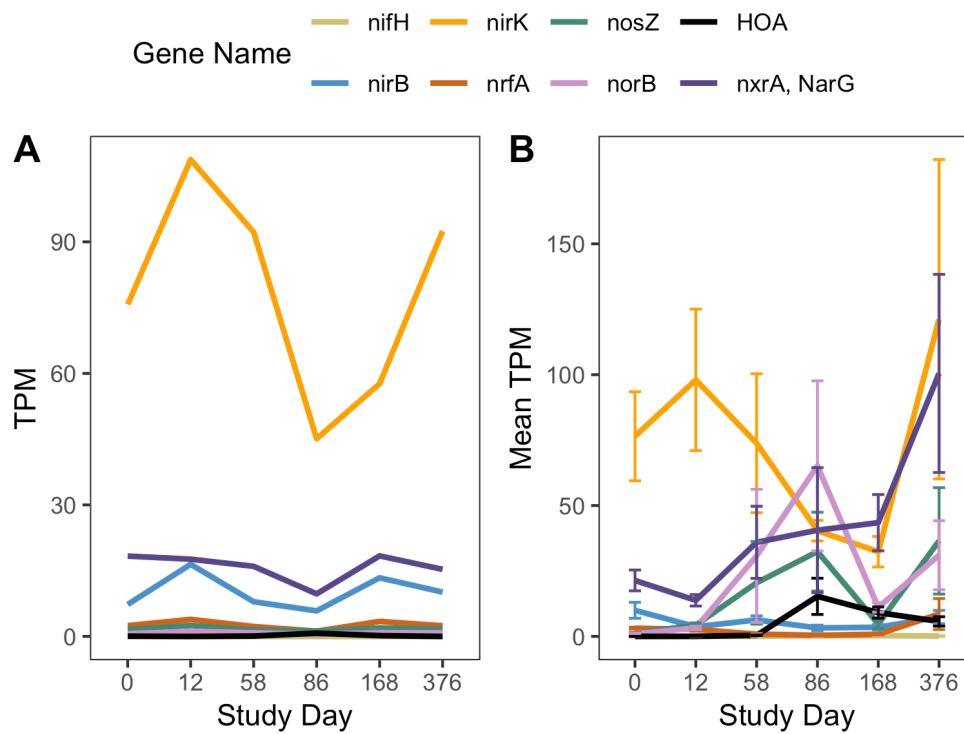


## Nitrogen- and sulfur-enriched molecules

Expression of nitrogen cycling genes was impacted in response to human decomposition. Due to the detection of *hao* in our differential expression analysis, and our hypotheses predicting changes to nitrogen transformation processes, the expression of genes encoding common enzymes involved in nitrogen cycling (*nifH*, *nirB*, *nirK*, *norB*, *nosZ*, *nrfA*, *nrrA*, and *amoA*) were assessed using their enzyme commission numbers (Fig 5A,B). *nifH*, encoding a subunit of nitrogenase which is involved in nitrogen fixation, displayed little to no changes in gene expression between control and decomposition soils. Transcripts for two genes encoding enzymes contributing to the last two steps of denitrification, *norB* (encodes nitric oxide reductase) and *nosZ* (encodes nitrous oxide reductase), increased between study days 12 and 86, and decreased at study day 168 before increasing again at day 376. In contrast, expression of genes encoding nitrate reductase, *narG*, and NO-forming nitrite reductase, *nirK*, remained low until day 376 when transcripts for both genes increased. As noted above, expression of *hao*, encoding hydroxylamine dehydrogenase, increased at study day 86 before decreasing at remaining timepoints (Fig 3A, Fig 5B). Expression of *amoA*, encoding a subunit of ammonia monooxygenase, and *nrrA*, encoding a subunit of nitrite oxidoreductase, which are involved in nitrification, changed in response to decomposition. *amoA* transcripts initially decreased at day 12, remaining reduced until study day 376. Similarly, abundance of genes that encode for enzymes involved in dissimilatory nitrate reduction, *nirB*, and *nrfA*, was low for the first 168 days, with *nrfA* expression increasing at day 376 (Fig 5B).

**Figure 5: Average gene expression, in transcripts per million (TPM), of commonly used marker genes for enzymes involved in nitrogen cycling over time in controls (A) and decomposition (B) soils.** Data in B represent mean and standard deviation of TPM from three individuals.

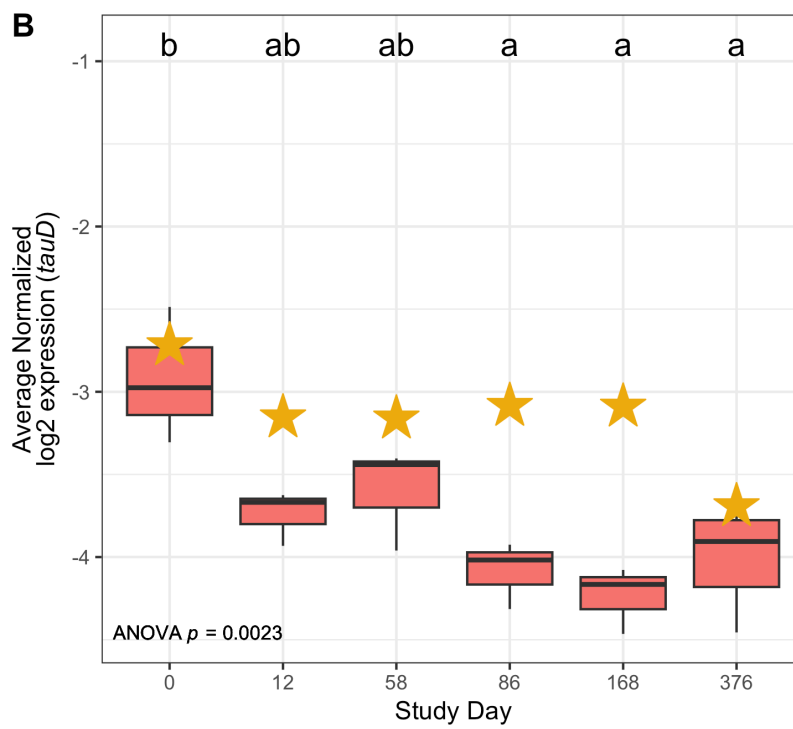
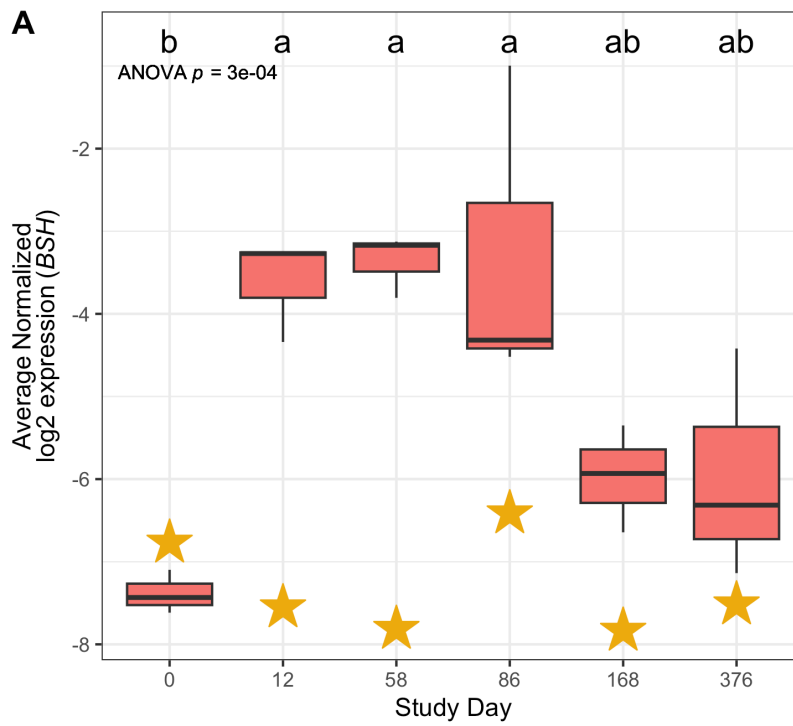




Expression of genes involved in metabolism of nitrogen and sulfur-containing compounds were also impacted by human decomposition. Specifically, four of the top ten genes whose expression decreased at day 12 were related to taurine metabolism, with their annotations associated with *tauD*, encoding taurine dioxygenase. (Supplementary Material 6). Further investigation into *tauD* showed that mean expression of these genes decreased steadily over one year, beginning at day 12 (Fig 6B); however, *tauD* expression in response to human decomposition was variable across taxonomic associations. Most *tauD* transcripts were associated with *Gammaproteobacteria*, *Actinobacteria*, *Betaproteobacteria*, *Alphaproteobacteria*, and fungi. While a majority of the *tauD* gene queries displayed reduced expression over time, expression of fungal-associated and a few *Betaproteobacteria*-associated *tauD* genes increased at day 58 (Supplementary Material 7). Sources of taurine in the human body include taurine

absorbed from the diet and taurine produced from anaerobic microbial deconjugation of bile salts via bile salt hydrolase (BSH) enzymes [23]. Therefore, we also looked at expression of genes encoding BSH enzymes in decomposition soils. Expression of these genes was elevated at days 12, 58, and 86 before converging toward pre-decomposition levels at days 168 and 376 (Fig 6A). Hierarchical liner mixed effects (HLM) models showed that both *tauD* (HLM  $F = 7.356$ ,  $p = 0.002$ ) and BSH ( $F = 13.768$ ,  $p < 0.001$ ) gene expression was significantly different over time (Fig 6A,B).

**Figure 6: Mean bile salt hydrolase, BSH, (A) and *tauD*, taurine dioxygenase, (B) log2 normalized expression in controls (gold stars) and decomposition (boxplots) soils.** Boxplots display the 25th and 75th quartiles and median log2 normalized values between all three individuals at each timepoint. ANOVA p-value is the result of a hierarchical linear mixed effects model accounting for repeated measures of each donor block, while letters denote the results of *post-hoc* Tukey test.



## Discussion

The goal of this study was to assess soil microbial gene expression in response to human decomposition. Metatranscriptomics were applied to soil samples collected over one year from below three decomposing human bodies. From this, we showed that microbial gene expression shifted over time, with samples reproducible between individuals. Additionally, we showed that gene expression profiles had not recovered to pre-decomposition conditions after one year. Comparison of control and decomposition expression profiles revealed that heat-shock proteins were elevated in response to decomposition. We also described expression patterns between decomposition time-points, noting changes in functional gene categories at certain timepoints, in particular with respect to lipid, nitrogen and sulfur metabolism.

### Gene expression patterns in decomposition soils

Gene expression profiles remained altered after one year of decomposition. It is unclear if soil microbial communities, in terms of gene expression profiles, have reached a new steady state as a result of decomposition, or if they would eventually return to pre-decomposition conditions. The parameters pH, EC,  $\text{NH}_4^+$ ,  $\text{NO}_3^-$ , and total nitrogen (TN) exhibited differences (although not statistical) in these soils following a year of decomposition, reflected by changes in beta diversity which also did not show community recovery [18]. This indicates that decomposition-derived materials present in the soil have not been fully cycled, and thus can continue to structure microbial communities and impact their function for extended periods of time. While nutrient pools and communities both demonstrate less rapid change at later time points in the study, there is not evidence suggesting an arrival at a steady-state post-disturbance microbial community. Further, Barton et al. (2020) [24] reported that soil phosphorus, nitrogen (total, ammonium, and nitrate), and electrical conductivity were still elevated above background levels after 500 days of human decomposition, suggesting

decomposition events have long lasting effects on the local ecosystem. Together, this has implications for terrestrial ecosystem processing (*e.g.*, nutrient cycling, emission of greenhouse gasses, etc.), as we show that decomposition alters functional metabolism pathways within soil microbial communities. Further work with extended sample collections beyond one year are needed to address how long microbial gene expression is impacted.

Bacteria, fungi, and archaea were all represented in expressed genes throughout decomposition, suggesting that members of all three domains have the potential to contribute to decomposition processes and nutrient cycling. While a majority of annotated transcripts were identified as bacteria, fungal transcripts were the second most abundant group. Fungal transcripts made up almost half (seven of the top 15) of the significantly differentially expressed genes associated with decomposition-impacted soils. Additionally, with respect to expression shifts between decomposition timepoints, fungal transcripts were among the topmost upregulated genes at study day 86. The presence of fungal transcripts is not surprising as fungi are key decomposers, involved in the degradation of organic matter in terrestrial ecosystems [25]. It was interesting to see an increase in certain fungal transcripts, such as lipase, at study days 58 and 86 when soil oxygen began to recover. We would expect lipids to enter the soil as tissues are broken down during decomposition, however this did not inform the expression pattern of bacterial lipase genes, as they decreased during decomposition. This suggests that microbial activity in decomposition soils may be constrained by the changing chemical environment, potentially altered oxygen levels in the case of lipase gene expression. Similarly, prior work with these soils showed a relationship between fungal community composition and soil oxygen [18], indicating that fungal communities underwent shifts in both community structure and activity in decomposition-impacted soils.

## 967 **Heat-shock/stress response**

968

969 Soil microbial communities expressed stress response genes in response to human  
970 decomposition. Differential expression analysis identified increased expression of mul-  
971 tiple heat shock proteins associated with the taxa *Xanthomonadales*, *Actinobacteria*,  
972 and fungi. Upon further investigation, expression of these genes increased through day  
973 58 and remained high for the remainder of the year. Soil temperature was elevated rel-  
974 ative to controls (up to 10°C higher) between study days 8 and 80, while soil electrical  
975 conductivity increased up to 663  $\mu\text{S}/\text{cm}$  (16X higher than background) through day  
976 58 before slowly decreasing through the remainder of the study. Soil electrical conduc-  
977 tivity (correlates with ionic strength [26] and can indicate soil salinity) has previously  
978 been shown to increase in decomposition soils [7–9, 18]. As a result, we would expect  
979 these microbes to be experiencing both heat and osmotic stress during this period.  
980 Prior work has observed increased heat shock gene expression during salt stress in  
981 paddy soils [27] and the presence of both heat and osmotic stress genes in desert soils  
982 along a salt gradient [28], suggesting saline conditions can alter the expression of heat  
983 and/or osmotic stress genes. In our study we observed that stress response within soil  
984 microbial communities is stimulated during human decomposition, however, at this  
985 time, it is unclear if expression of these genes is in response to heat stress alone, or in  
986 combination with osmotic stress.

999

## 1000 **Carbon-containing compounds**

1001

1002 Human fat tissue contains lipids that are broken down during decomposition. There-  
1003 fore, we assessed expression of triacylglycerol lipase genes in decomposition soils. Our  
1004 results show that expression of triacylglycerol lipase genes was altered in response to  
1005 decomposition, and these shifts differed between bacterial and fungal transcripts. Bac-  
1006 terial triacylglycerol lipase transcripts decreased in response to decomposition, while  
1007 fungal triacylglycerol lipase transcripts increased. These results suggest that fungi  
1008

may be important triacylglycerol degraders in human decomposition-impacted soils. Further, expression of these genes corresponded to changes in relative abundance of the fungal classes *Saccharomycetes*, *Sordariomycetes*, and *Eurotiomycetes* [18]. These fungi have been previously associated with decomposition soils [15, 17] and are known to contain triacylglycerol lipase genes in their genomes [29, 30], suggesting that these organisms are important for lipid degradation in decomposition soils.

Our observation of an overall decrease in triacylglycerol lipase transcripts contrasts with previous work by Howard et al. (2010) [22], who observed increased gene copy number of Group 1 lipase genes via qPCR during swine decomposition. Fatty acid composition differs in human compared to pig tissue [31], potentially altering the lipid profile available for microbes, leading to differences in decomposition products within the soil [21]. These products can then directly or indirectly alter community composition and/or activity of functional proteins via substrate availability or the chemical environment. Further, decomposition of humans and pigs resulted in increased pH in soils below pigs, and decreased pH below humans [21]. Altered pH and soil chemistry could result in a different functional potential and/or gene expression in decomposition-impacted soils, especially as it relates to lipase genes, as many triacylglycerol lipases have a pH optimum that is neutral to basic [32–34], so cells may be decreasing expression under acidic conditions in human decomposition soils. Availability of lipid species and changes to pH may select for taxa that favor these substrates/pH conditions; for example, Mason et al. (2022) [11] suggested the abundance of the fungal taxa *Saccharomycetes* was related to antemortem BMI due to relative proportions of fat and muscle tissue.

## Nitrogen enriched compounds/N-cycling

The human body is a concentrated source of nitrogen that is released into the surrounding soil during decomposition, therefore we also evaluated expression of genes involved

1059 in nitrogen cycling. Expression of common marker genes for nitrogen cycling was  
 1060 altered in decomposition soil and suggested nitrogen transformations during human  
 1061 decomposition are driven by soil oxygen concentrations with hydroxylamine as an  
 1062 important intermediate. We observed low or reduced expression of nitrification genes  
 1063 *nrrA* and *amoA* between days 12 and 86, during a period when oxygen was reduced to  
 1064 39% - 85%. This was concomitant with accumulation of ammonium, which reached a  
 1065 maximum on day 12, and low nitrate conditions indicating that nitrification was inhib-  
 1066 ited. This period of reduced soil oxygen constraining nitrification was also described  
 1067 in a decomposition experiment with beaver carcasses Keenan et al. (2018) [7].  
 1068 We observed increased expression of *hao*, which encodes the enzyme hydroxylamine  
 1069 dehydrogenase (HAO) at day 86 while oxygen was reduced (~85%). This corresponded  
 1070 to simultaneous increases in expression of genes encoding nitric oxide reductase (*norB*)  
 1071 and nitrous oxide reductase (*nosZ*). Traditionally HAO has been thought to pro-  
 1072 cess hydroxylamine to nitrite during nitrification, while NorB and NosZ are enzymes  
 1073 involved in the last two steps of denitrification converting nitric oxide (NO) to dini-  
 1074 trogen gas (N<sub>2</sub>). However, recent work has suggested hydroxylamine can be converted  
 1075 to nitric oxide (NO), as well as can interact with multiple phases of the nitrogen cycle  
 1076 [35]. Even though *amoA* expression was shown to decrease during reduced oxygen  
 1077 conditions, *amoA* transcripts were still present and likely able to convert ammonium  
 1078 to hydroxylamine as soil oxygen was not completely depleted during decomposition.  
 1079 Additionally, a previous study reported that the growth of the ammonia oxidizing  
 1080 bacteria *Nitrosomonas europaea* under anoxic conditions lead to accumulation of  
 1081 hydroxylamine in a chemostat bioreactor [36], suggesting anaerobic ammonium oxi-  
 1082 dation (anammox) may also be occurring in decomposition soils. However, we did  
 1083 not observe increases in *nirK* expression, which might suggest conversion of nitrite to  
 1084 NO for use in the anammox pathway. NO produced via HAO activity may be used  
 1085 for anammox in these soils; however, the role of hydroxylamine as an intermediate  
 1086



in anammox is still debated [35]. Therefore, our current hypothesis is that hydroxylamine accumulates under anaerobic conditions during decomposition, which can then be converted to NO by HAO. This NO would then be present for anaerobic denitrifying bacteria to convert to nitrous oxide (N<sub>2</sub>O) by NorB and finally to N<sub>2</sub> by NosZ. Keenan et al. (2018) [7] also noted a brief increase in N<sub>2</sub>O emissions, which suggests denitrification was occurring during this phase of reduced soil oxygen concentrations.

As soils fully reoxygenated by day 168, we observed increased expression of genes encoding enzymes involved in aerobic nitrification, *amoA* and *nxrR*. Nitrification is an oxygen-dependent process which would be converting the accumulated ammonium to nitrate; the increase in nitrate concentrations may then serve as a substrate for denitrification. We observed increased expression of marker genes encoding all four enzymes in the complete dissimilatory denitrification pathway (*narG*, *nirK*, *norB*, and *nosZ*) at day 376. Increased expression of nitrification and denitrification marker genes is consistent with accumulation of nitrite, nitrate, and N<sub>2</sub>O after oxygen is reintroduced to soils described in Keenan et al. (2018) [7]. Together, gene expression patterns in our study provide further insight into nitrogen transformations in during vertebrate decomposition, suggesting an important role of hydroxylamine.

## Sulfur-containing compounds

Sulfur is present in various organic molecules, including taurine, a sulfur- and nitrogen-containing acid involved in bile acid formation [23]. Taurine is present in the human body, where it can be absorbed from the diet or synthesized in the liver [37]. However, taurine is also produced as a byproduct of the deconjugation of bile salts via bile salt hydrolases (BSH) present in the anaerobic gut taxa *Lactobacillus* and *Clostridium* [23]. In our study, we observed increased expression of genes encoding BSH enzymes between days 12 and 86. Given that increased expression of BSH genes corresponded to the beginning of active decomposition, when decomposition products were observed

1151 to enter the soil, and the period of reduced dissolved oxygen in our study, it is likely  
1152 that taurine accumulation is the result of BSH enzyme activity by anaerobic microor-  
1153 ganisms. While we did not measure taurine concentrations in this study, our results  
1154 correspond to previous decomposition studies that report accumulation of taurine  
1155 in various organs and body regions [38–40] and soils [21, 41] during decomposition  
1156 via metabolomics, and increased relative abundance of *Clostridium* and *Lactobacillus*  
1157 within the body [42–44] and in decomposition soils [12] via DNA sequencing methods,  
1158 including in these soils [18].

1164  
1165 One pathway of taurine metabolism is through desulfurization via the  $\alpha$ -ketoglutarate-  
1166 dependent enzyme taurine dioxygenase (TauD). Specifically, this enzyme, encoded  
1167 by the gene *tauD*, converts 2-oxoglutarate and taurine to produce aminoacetalde-  
1168 hyde, succinate, sulfite, and CO<sub>2</sub> [45]. Succinate and sulfite from this reaction can  
1169 then be used for the citric acid cycle and sulfur metabolism, respectively. Given  
1170 increased BSH expression in our study and reported taurine accumulation in others,  
1171 we would expect taurine to be present for microbial metabolism by TauD. How-  
1172 ever, we observed a general decrease in *tauD* expression between days 12 through  
1173 376. This trend was driven by reduced expression of *tauD* transcripts associated  
1174 with *Proteobacteria*, *Gammaproteobacteria*, and *Actinobacteria* whose relative abun-  
1175 dance have been shown to remain consistent or increase during human decomposition  
1176 [12], suggesting that *tauD* expression is downregulated under decomposition condi-  
1177 tions. However, we noted that expression of *tauD* genes associated with fungi and  
1178 a few *Betaproteobacteria* displayed increased expression at day 58, corresponding to  
1179 increased expression of bile salt hydrolases (BSH) between days 12 and 86. The reduc-  
1180 tion in *tauD* expression may be due to sulfur availability. We did not measure sulfur  
1181 species in this experiment; however, others have observed increased sulfur concentra-  
1182 tions in decomposition-impacted soils [6, 10, 46]. Thus, sulfur scavenging pathways  
1183  
1184  
1185  
1186  
1187  
1188  
1189  
1190  
1191  
1192  
1193  
1194  
1195  
1196

such as taurine desulfurization by TauD [47], whose genes are expressed under sulfur-limiting conditions, likely display reduced expression under sulfur replete conditions. Additionally, taurine may be processed through other pathways. For example, taurine can be deaminated by taurine dehydrogenase to produce sulfite and acetyl-CoA for carbon metabolism [45, 48]. Overall, our results suggest that human decomposition has potential impacts on soil sulfur biogeochemistry through deposition of inorganic (sulfate) and organic (sulfur-containing amino acids) sulfur compounds.

## Conclusion

This study represents the first investigation of soil microbial gene expression during human decomposition. Metatranscriptomic analysis of soils from three human individuals over one year shows that decomposition impacted microbial community gene expression profiles, exhibiting functional shifts over time. This included altered expression of genes involved in lipid, N and S metabolism as microbes processed the nutrient-rich tissues of the human body. Additionally, we noted that functionality within decomposition-impacted soils was still affected after one year and had not returned to starting or background conditions. Together, these results show that vertebrate decomposition has lasting impacts on local soil ecosystems, including soil microbial communities. These results have important implications for understanding biogeochemical changes due to vertebrate mortality events in terrestrial ecosystems.

## Materials and Methods

### Study design

In February 2018, three deceased male human subjects (hereafter, “donors”) were placed supine on the soil surface at the University of Tennessee Anthropology Research Facility (ARF) and allowed to decompose. Located in Knoxville, TN (35° 56’ 28” N,

1243 83° 56' 25" W) the ARF is a roughly 2-acre outdoor facility dedicated to studying  
1244 human decomposition [13]. The soils at the ARF are comprised of the Loyston-Talbott-  
1245 Rock outcrop (LtD) and Coghill-Corryton (CcD) complexes. LtD soils are a silty clay  
1246 loam and channery clay overlaying lithic bedrock, while CcD soils are comprised of  
1247 clay from weathered quartz limestone [13, 18]. A site that had not been previously  
1248 exposed to decomposition was used for this study.

1249  
1250  
1251  
1252  
1253 The decomposition field experiment is fully described in Taylor et al. (2024) [18].  
1254 Briefly, experiments were conducted in a block design, where each block consisted of  
1255 one decomposition site and one control site [18]. In total three blocks, *i.e.*, three donors  
1256 paired with three respective control sites, were included in the study. Each control site  
1257 was chosen in a manner to ensure their location was uphill and roughly 2 m away from  
1258 decomposition sites [18]. Donor internal temperatures were recorded by probes located  
1259 in the abdomen, while ambient air temperatures were monitored via sensors located  
1260 roughly 50 cm above the soil surface. Soil temperature and salinity were measured  
1261 with sensors placed directly underneath each individual (Decagon Devices, GS3) [18].  
1262 Donor ages ranged from 65 to 86 and were within 1 kg of each other with regard to  
1263 weight (90.7 to 91.6 kg); donor BMI varied between 27.7 to 29.6 [18].

## 1273 **Sampling and physiochemistry**

1274  
1275 Decomposition of all subjects was observed for one year. During the one-year study  
1276 period, soils were sampled at 20 timepoints chosen to correspond with morphological  
1277 stages of decomposition as described by [49]. Once advanced decay was reached, soils  
1278 were collected at intervals of 350 accumulated degree days (ADD), calculated using  
1279 ambient air temperatures, up to one year. All soil cores were taken using a 1.9 cm  
1280 (3/4 inch) diameter soil auger to a depth of 16 cm. Soils were divided into two depth  
1281 fractions: 0-1 cm (interface) and 1-16 cm (core) for the analyses reported in Taylor et  
1282  
1283  
1284  
1285  
1286  
1287  
1288

al. (2024) [18]; the entire 0 to 16 cm core was used for this current study. Decomposition soils were taken from directly beneath the cadavers, taking care to not re-sample the same location more than once. At the time of sampling, soil dissolved oxygen was measured in triplicate using an Orion Star™ A329 pH/ISE/Conductivity/Dissolved Oxygen portable multiparameter meter (ThermoFisher) [18].

A subset of 6 study timepoints were chosen for metatranscriptomics analysis. Study days 0, 12, 58, 86, 168, and 376 were chosen as they represented distinct morphological and soil biogeochemical stages during decomposition. Study day 0 was chosen as a baseline sample prior to cadaver placement. Study day 12 was chosen as this was the start of active decomposition and corresponded to maximum soil ammonium concentrations and minimum soil oxygen (approximately 39%). Study day 58 was chosen as this sample represented the pH minimum, and respiration and soil temperature were at a maximum [18]. Additionally, ammonium concentrations began to decrease around day 58. Study day 86 was chosen as the time period when soil oxygen started to recover and nitrate levels began to increase. Study day 168 was chosen as nitrate was at its maximum and soil dissolved oxygen had returned to 99%. Finally, day 376 was chosen to represent the end of the study, approximately 1 year since cadaver placement. Each study day was represented by four soil samples for RNA extraction: one pooled control sample which was a mix of the three control locations, plus one sample from each of the three donors, yielding a total of 24 samples for this study.

Soil samples were transported back to the lab at the University of Tennessee (Knoxville, TN) and processed within 24 hours of collection. Soils were homogenized by hand to remove insect larvae, roots, rocks, and other debris (> 2 mm). A subset of soils were used to measure pH, electrical conductivity (EC), and evolved CO<sub>2</sub> as described in Taylor (2020). Soil nitrogen species (NH<sub>4</sub><sup>+</sup>, NO<sub>3</sub><sup>-</sup>) and total carbon (TC) and nitrogen (TN) were measured in all soil samples as described in [18]. Reported

values for soil physiochemistry represent the full 16 cm core; estimated by summing interface and core values reported by Taylor et. al, (2024) [18] in 1:16 and 15:16 ratios, respectively. Control reported here are means of the three experimental controls that were unimpacted by decomposition.

Roughly 10 g of soil was reserved for nucleic acid extraction, placed in a 4 oz. Whirl-Pak™ bag (Nasco), and flash frozen in liquid nitrogen. All samples were stored at -80°C until further analysis. Bacterial and fungal community composition was assessed via amplicon sequencing of the 16S rRNA gene and ITS2 region as described in Taylor et al. (2024).

## **RNA Extraction and Sequencing**

RNA was extracted from 2 g of soil using Qiagen's RNeasy® PowerSoil® Total RNA kit (catalog no. 12866-25). Manufacturer's instructions were followed with a few modifications. Soils became saline during decomposition; therefore, we followed manufacturer's suggestion and incubated all extracts at -20°C following addition of solution SR4 (step 9) to decrease salt precipitation. All RNA samples were resuspended in 40 µl of Solution SR7. RNA concentrations were assessed fluorometrically using the Qubit® RNA HS assay (catalog no. Q32852) with 1 µl of RNA. DNA contamination was removed by DNase treating RNA extracts twice using Qiagen's DNase Max® kit in 50 µl reactions. RNA concentrations were remeasured after DNase treatment. PCR with general V4 16S rRNA gene primers [50, 51] was conducted using RNA extracts as the template to confirm removal of all DNA prior to sequencing. RNA aliquots were shipped to HudsonAlpha Discovery (Huntsville, AL) for library preparation and RNA sequencing. Dual-indexed libraries were prepared using the Illumina® Stranded Total RNA prep with ribosomal RNA depletion via ligation with Ribo-Zero Plus. Libraries were then pooled and sequenced on Illumina's NovaSeq 6000 v4 platform, resulting in demultiplexed fastq files for each sample.

## Bioinformatics

Read quality control (QC) was conducted in KBase [52] using Trimmomatic [53]. Paired fastq files were imported to KBase through Globus. Poor quality reads were removed, and adapters trimmed via Trimmomatic (v0.36) using default settings and the TruSeq3-PE-2 adapter file. After QC check with FastQC, trimmed libraries were exported as fastq files from KBase through Globus. Remaining ribosomal RNA was filtered using bbmap (maxindel = 20, minid = 0.93) from the Joint Genome Institute's (JGI) bbtools suite [54]. After this step, all non-ribosomal reads from all 24 samples were merged into one file. This file was then used to co-assemble reads into contigs using the de novo assembler MEGAHIT (v1.2.9) [55] (-12 -k-min 23, -k-max 123, -k-step 10).

Gene identification and annotation from co-assembled contigs was performed using Prodigal [56] and eggNOG mapper [57], respectively. Briefly, the fastq containing all contigs was submitted to Prodigal (v2.6.3) for protein coding gene predication for a meta-sample (-p meta -f gff). Next, predicated genes were functionally and taxonomically annotated using eggNOG mapper (v2.1.6) using basic settings to perform a diamond blastp search [58]. Only genes that were both functionally and taxonomically annotated by one of the databases used by eggNOG mapper and identified as bacterial, archaeal, or fungal were chosen as genes of interest. Transcript counts for all genes of interest were obtained by mapping reads from each respective sample to genes of interest obtained from co-assembly using QIAGEN CLC Genomics Workbench 20.0 (<https://digitalinsights.qiagen.com/>).

## Differential Expression

Transcript counts from all samples were combined in a single workable data file and imported into R for differential expression analysis using the R packages edgeR [59] and limma [60] following a modified pipeline by Phipson et al. (2020) [61]. Briefly,

the transcript count table was imported into R and converted to a DGElist object. Genes without sufficient counts for statistical analysis were removed to increase power using the edgeR function filterByExpr(). Raw counts were then log2 normalized and gene expression profiles compared via multidimensional scaling (MDS) and hierarchical clustering. For differential expression analysis, raw filtered reads were normalized using edgeR's trimmed mean of M values (TMM) normalization using the function calcNormFactors(). TMM normalized reads were then log2 transformed using limma's voom() and differential expression assessed. Empirical Bayes shrinkage was used correct to p-values for false discovery rates. The topmost up and down regulated genes for each comparison, determined by log2 fold change and adjusted p-values, were then reported. Expression of certain genes were assessed after performing transcripts per million (TPM) normalization and statistical analyses with a combination of analysis of variance (ANOVA) and post-hoc Tukey tests. ANOVA across all timepoints were applied to hierarchical linear mixed effects models to account for repeated sampling within each donor block.

## Availability of data and materials

RNA sequence files from the Novoseq instrument can be found at XXXX. The datasets supporting the conclusions of this article are available at the GitHub repository [Mason\\_MetaT\\_XXX\\_2024](#)."

## References

- [1] Benninger, L. A., Carter, D. O. & Forbes, S. L. The biochemical alteration of soil beneath a decomposing carcass. *Forensic Science International* **180**, 70–5 (2008).
- [2] Towne, E. G. Prairie vegetation and soil nutrient responses to ungulate carcasses. *Oecologia* **122**, 232–239 (2000). URL <https://doi.org/10.1007/PL00008851>.



- [3] Parmenter, R. R. & MacMahon, J. A. Carrion decomposition and nutrient cycling in a semiarid shrub–steppe ecosystem. *Ecological Monographs* **79**, 637–661 (2009).
- [4] Macdonald, B. C. T. *et al.* Carrion decomposition causes large and lasting effects on soil amino acid and peptide flux. *Soil Biology and Biochemistry* **69**, 132–140 (2014).
- [5] Bump, J. K. *et al.* Ungulate Carcasses Perforate Ecological Filters and Create Biogeochemical Hotspots in Forest Herbaceous Layers Allowing Trees a Competitive Advantage. *Ecosystems* **12**, 996–1007 (2009).
- [6] Aitkenhead-Peterson, J. A., Owings, C. G., Alexander, M. B., Larison, N. & Bytheway, J. A. Mapping the lateral extent of human cadaver decomposition with soil chemistry. *Forensic Science International* **216**, 127–34 (2012).
- [7] Keenan, S. W., Schaeffer, S. M., Jin, V. L. & DeBruyn, J. M. Mortality hotspots: nitrogen cycling in forest soils during vertebrate decomposition. *Soil Biology and Biochemistry* **121**, 165–176 (2018).
- [8] Fancher, J. P. *et al.* An evaluation of soil chemistry in human cadaver decomposition islands: Potential for estimating postmortem interval (PMI). *Forensic Science International* **279**, 130–139 (2017).
- [9] Quaggiotto, M.-M., Evans, M. J., Higgins, A., Strong, C. & Barton, P. S. Dynamic soil nutrient and moisture changes under decomposing vertebrate carcasses. *Biogeochemistry* **146**, 71–82 (2019).
- [10] Taylor, L. S. *et al.* Soil elemental changes during human decomposition. *PLoS ONE* **18**, 1–24 (2023). URL <https://doi.org/10.1371/journal.pone.0287094>. Publisher: Public Library of Science.

1519 [11] Mason, A. R. *et al.* Body mass index (BMI) impacts soil chemical and microbial  
1520 response to human decomposition. *mSphere* **0**, e0032522 (2022).  
1521  
1522  
1523 [12] Cobough, K. L., Schaeffer, S. M. & DeBruyn, J. M. Functional and structural  
1524 succession of soil microbial communities below decomposing human cadavers.  
1525 *PLoS One* **10**, e0130201 (2015).  
1526  
1527  
1528  
1529 [13] Keenan, S. W. *et al.* Spatial impacts of a multi-individual grave on microbial  
1530 and microfaunal communities and soil biogeochemistry. *PLoS One* **13**, e0208845  
1531 (2018).  
1532  
1533  
1534  
1535 [14] Singh, B. *et al.* Temporal and spatial impact of human cadaver decomposition  
1536 on soil bacterial and arthropod community structure and function. *Frontiers in*  
1537 *Microbiology* **8**, 2616 (2018).  
1538  
1539  
1540  
1541 [15] Metcalf, J. L. *et al.* Microbial community assembly and metabolic function during  
1542 mammalian corpse decomposition. *Science* **351**, 158–62 (2016).  
1543  
1544  
1545 [16] Finley, S. J., Pechal, J. L., Benbow, M. E., Robertson, B. K. & Javan, G. T. Micro-  
1546 bial Signatures of Cadaver Gravesoil During Decomposition. *Microbial Ecology*  
1547 **71**, 524–529 (2016).  
1548  
1549  
1550  
1551 [17] Fu, X. *et al.* Fungal succession during mammalian cadaver decomposition and  
1552 potential forensic implications. *Scientific Reports* **9**, 12907 (2019).  
1553  
1554  
1555 [18] Taylor, L. S. *et al.* Soil microbial communities and biogeochemistry during human  
1556 decomposition differs between seasons: evidence from year-long trials (2024).  
1557 URL <https://www.researchsquare.com/article/rs-3931135/v1>.  
1558  
1559  
1560  
1561 [19] Burcham, Z. M. *et al.* Total RNA analysis of bacterial community structural  
1562 and functional shifts throughout vertebrate decomposition. *Journal of Forensic*  
1563  
1564

	<i>Sciences</i> <b>64</b> , 1707–1719 (2019).	1565
		1566
[20]	Ashe, E. C., Comeau, A. M., Zejdlik, K. & O’Connell, S. P. Characterization of	1567
	bacterial community dynamics of the human mouth throughout decomposition	1568
	via metagenomic, metatranscriptomic, and culturing techniques. <i>Frontiers in</i>	1569
	<i>Microbiology</i> <b>12</b> , 689493 (2021).	1570
		1571
		1572
		1573
		1574
[21]	DeBruyn, J. M. <i>et al.</i> Comparative decomposition of humans and pigs: soil biogeo-	1575
	chemistry, microbial activity and metabolomic profiles. <i>Frontiers in Microbiology</i>	1576
	<b>11</b> , 608856 (2021).	1577
		1578
		1579
		1580
[22]	Howard, G. T., Duos, B. & Watson-Horzelski, E. J. Characterization of the	1581
	soil microbial community associated with the decomposition of a swine carcass.	1582
	<i>International Biodeterioration &amp; Biodegradation</i> <b>64</b> , 300–304 (2010).	1583
		1584
		1585
		1586
[23]	Urdaneta, V. & Casadesús, J. Interactions between Bacteria and Bile Salts in	1587
	the Gastrointestinal and Hepatobiliary Tracts. <i>Frontiers in Medicine</i> <b>4</b> (2017).	1588
		1589
		1590
[24]	Barton, P. S. <i>et al.</i> Soil chemical markers distinguishing human and pig decom-	1591
	position islands: a preliminary study. <i>Forensic Science, Medicine and Pathology</i>	1592
	(2020).	1593
		1594
		1595
		1596
[25]	van der Wal, A., Geydan, T. D., Kuyper, T. W. & de Boer, W. A thready affair:	1597
	linking fungal diversity and community dynamics to terrestrial decomposition	1598
	processes. <i>FEMS Microbiology Reviews</i> <b>37</b> , 477–494 (2013).	1599
		1600
		1601
		1602
[26]	Essington, M. E. <i>Soil and water chemistry: an integrative approach</i> (CRC press,	1603
	2015).	1604
		1605
		1606
[27]	Peng, J., Wegner, C.-E. & Liesack, W. Short-Term Exposure of Paddy Soil Micro-	1607
	bial Communities to Salt Stress Triggers Different Transcriptional Responses of	1608
		1609
		1610

1611 Key Taxonomic Groups. *Frontiers in Microbiology* **8** (2017).  
1612  
1613 [28] Pandit, A. S. *et al.* A snapshot of microbial communities from the Kutch: one of  
1614 the largest salt deserts in the World. *Extremophiles* **19**, 973–987 (2015).  
1615  
1616 [29] Dujon, B. *et al.* Genome evolution in yeasts. *Nature* **430**, 35–44 (2004).  
1617  
1618 [30] Haridas, S. *et al.* The genome and transcriptome of the pine saprophyte *Ophios-*  
1619 *toma piceae*, and a comparison with the bark beetle-associated pine pathogen  
1620 *Grosmannia clavigera*. *BMC Genomics* **14**, 373 (2013).  
1621  
1622 [31] Notter, S. J., Stuart, B. H., Rowe, R. & Langlois, N. The Initial Changes of  
1623 Fat Deposits During the Decomposition of Human and Pig Remains. *Journal of*  
1624 *Forensic Sciences* **54**, 195–201 (2009).  
1625  
1626 [32] Kok, R. G. *et al.* Characterization of the extracellular lipase, LipA, of *Acineto-*  
1627 *bacter calcoaceticus* BD413 and sequence analysis of the cloned structural gene.  
1628 *Molecular Microbiology* **15**, 803–818 (1995).  
1629  
1630 [33] Hasan, F., Shah, A. A. & Hameed, A. Influence of culture conditions on lipase  
1631 production by *Bacillus* sp. FH5. *Annals of Microbiology* **56**, 247–252 (2006).  
1632  
1633 [34] Zouaoui, B. & Bouziane, A. Production, optimization and characterization of  
1634 the lipase from *Pseudomonas aeruginosa*. *Romanian Biotechnological Letters* **17**,  
1635 7187–7193 (2012).  
1636  
1637 [35] Soler-Jofra, A., Pérez, J. & van Loosdrecht, M. C. M. Hydroxylamine and the  
1638 nitrogen cycle: A review. *Water Research* **190**, 116723 (2021).  
1639  
1640 [36] Yu, R., Perez-Garcia, O., Lu, H. & Chandran, K. *Nitrosomonas europaea* adapta-  
1641 tion to anoxic-oxic cycling: Insights from transcription analysis, proteomics and  
1642 metabolic network modeling. *Science of the Total Environment* **615**, 1566–1573  
1643  
1644  
1645  
1646  
1647  
1648  
1649  
1650  
1651  
1652  
1653  
1654  
1655  
1656

- (2018). 1657  
1658
- [37] Seidel, U., Huebbe, P. & Rimbach, G. Taurine: A Regulator of Cellular Redox 1659  
Homeostasis and Skeletal Muscle Function. *Molecular Nutrition & Food Research* 1660  
**63**, 1800569 (2019). 1661  
1662  
1663  
1664
- [38] Mora-Ortiz, M., Trichard, M., Oregioni, A. & Claus, S. P. Thanatometabolomics: 1665  
introducing NMR-based metabolomics to identify metabolic biomarkers of the 1666  
time of death. *Metabolomics* **15**, 37 (2019). 1667  
1668  
1669  
1670
- [39] Locci, E. *et al.* A <sup>1</sup>H NMR metabolomic approach for the estimation of the time 1671  
since death using aqueous humour: an animal model. *Metabolomics* **15**, 76 (2019). 1672  
1673  
1674
- [40] Zelentsova, E. A. *et al.* Post-mortem changes in the metabolomic compositions 1675  
of rabbit blood, aqueous and vitreous humors. *Metabolomics* **12**, 172 (2016). 1676  
1677  
1678
- [41] Hoeland Katharina, M. *Investigating the potential of postmortem metabolomics* 1679  
*in mammalian decomposition studies in outdoor settings*. Ph.D. thesis, University 1680  
of Tennessee-Knoxville, [https://trace.tennessee.edu/utk\\_graddiss/7000](https://trace.tennessee.edu/utk_graddiss/7000) (2021). 1681  
1682  
1683  
1684
- [42] Javan, G. T. *et al.* Human thanatomicrobiome succession and time since death. 1685  
*Scientific Reports* **6**, 29598 (2016). 1686  
1687  
1688
- [43] Javan, G. T., Finley, S. J., Smith, T., Miller, J. & Wilkinson, J. E. Cadaver 1689  
thanatomicrobiome signatures: the ubiquitous nature of Clostridium species in 1690  
human decomposition. *Frontiers in Microbiology* **8**, 2096 (2017). 1691  
1692  
1693  
1694
- [44] DeBruyn, J. M. & Hauther, K. A. Postmortem succession of gut microbial 1695  
communities in deceased human subjects. *PeerJ* **5**, e3437 (2017). 1696  
1697  
1698
- [45] Cook, A. M. & Denger, K. Metabolism of taurine in microorganisms. *Taurine* **6** 1699  
3–13 (2006). 1700  
1701  
1702

1703 [46] Vass, A. A., Bass, W. M., Wolt, J. D., Foss, J. E. & Ammons, J. T. TIME  
1704 SINCE DEATH DETERMINATIONS OF HUMAN CADAVERS USING SOIL  
1705 SOLUTION. *Journal of Forensic Sciences* **37**, 1236–1253 (1992).  
1706  
1707  
1708  
1709 [47] Kertesz, M. A. Riding the sulfur cycle – metabolism of sulfonates and sul-  
1710 fate esters in Gram-negative bacteria. *FEMS Microbiology Reviews* **24**, 135–175  
1711 (2000).  
1712  
1713  
1714 [48] Brüggemann, C., Denger, K., Cook, A. M. & Ruff, J. Enzymes and genes of  
1715 taurine and isethionate dissimilation in *Paracoccus denitrificans*. *Microbiology*  
1716 (*Reading, England*) **150**, 805–816 (2004).  
1717  
1718  
1719  
1720 [49] Payne, J. A. A summer carrion study of the baby pig *Sus Scrofa* Linnaeus.  
1721 *Ecology* **46**, 592–602 (1965).  
1722  
1723  
1724 [50] Apprill, A., McNally, S., Parsons, R. & Weber, L. Minor revision to V4 region SSU  
1725 rRNA 806R gene primer greatly increases detection of SAR11 bacterioplankton.  
1726 *Aquatic Microbial Ecology* **75**, 129–137 (2015).  
1727  
1728  
1729  
1730 [51] Parada, A. E., Needham, D. M. & Fuhrman, J. A. Every base matters: assessing  
1731 small subunit rRNA primers for marine microbiomes with mock communities,  
1732 time series and global field samples. *Environmental Microbiology* **18**, 1403–14  
1733 (2016).  
1734  
1735  
1736  
1737  
1738 [52] Arkin, A. P. *et al.* KBase: The United States Department of Energy Systems  
1739 Biology Knowledgebase. *Nature Biotechnology* **36**, 566–569 (2018).  
1740  
1741  
1742 [53] Bolger, A. M., Lohse, M. & Usadel, B. Trimmomatic: a flexible trimmer for  
1743 Illumina sequence data. *Bioinformatics* **30**, 2114–2120 (2014).  
1744  
1745  
1746 [54] Bushnell, B. BBMap.  
1747  
1748

- [55] Li, D., Liu, C.-M., Luo, R., Sadakane, K. & Lam, T.-W. MEGAHIT: an ultra-fast  
single-node solution for large and complex metagenomics assembly via succinct  
de Bruijn graph. *Bioinformatics* **31**, 1674–1676 (2015).
- [56] Hyatt, D. *et al.* Prodigal: prokaryotic gene recognition and translation initiation  
site identification. *BMC Bioinformatics* **11**, 119 (2010).
- [57] Cantalapiedra, C. P., Hernández-Plaza, A., Letunic, I., Bork, P. & Huerta-Cepas,  
J. eggNOG-mapper v2: Functional Annotation, Orthology Assignments, and  
Domain Prediction at the Metagenomic Scale. *Molecular Biology and Evolution*  
**38**, 5825–5829 (2021).
- [58] Buchfink, B., Reuter, K. & Drost, H.-G. Sensitive protein alignments at tree-of-  
life scale using DIAMOND. *Nature Methods* **18**, 366–368 (2021).
- [59] Robinson, M. D., McCarthy, D. J. & Smyth, G. K. edgeR: a Bioconduc-  
tor package for differential expression analysis of digital gene expression data.  
*Bioinformatics* **26**, 139–140 (2010).
- [60] Smyth, G. K. in *limma: Linear Models for Microarray Data* (eds Gentleman,  
R., Carey, V. J., Huber, W., Irizarry, R. A. & Dudoit, S.) *Bioinformatics and  
Computational Biology Solutions Using R and Bioconductor* 397–420 (Springer  
New York, New York, NY, 2005).
- [61] Phipson, B. *et al.* Differential expression analysis (2020).

## Acknowledgements

We would like to thank the Forensic Anthropology Center at the University of  
Tennessee-Knoxville for their help in setting up field experiments. We would like to  
thank Mary Davis for her help in managing the field site and helping to obtain donors

1795 for this work. This research was funded by a National Institute of Justice Award  
1796  
1797 (DOJ-NIJ-2017-R2-CX-0008) to LST and JMD.

1798

1799

## 1800 **Supplementary Information**

1801

1802

1803

1804

1805

1806

1807

1808

1809

1810

1811

1812

1813

1814

1815

1816

1817

1818

1819

1820

1821

1822

1823

1824

1825

1826

1827

1828

1829

1830

1831

1832

1833

1834

1835

1836

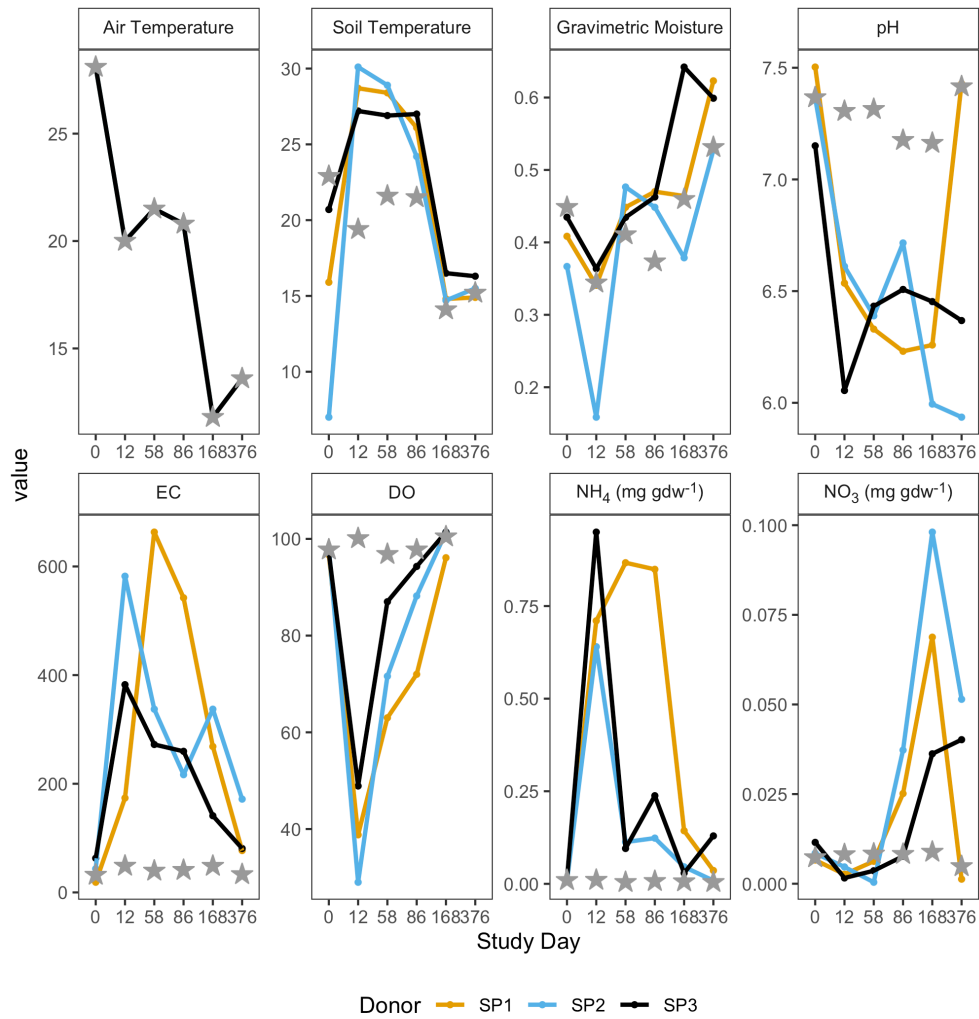
1837

1838

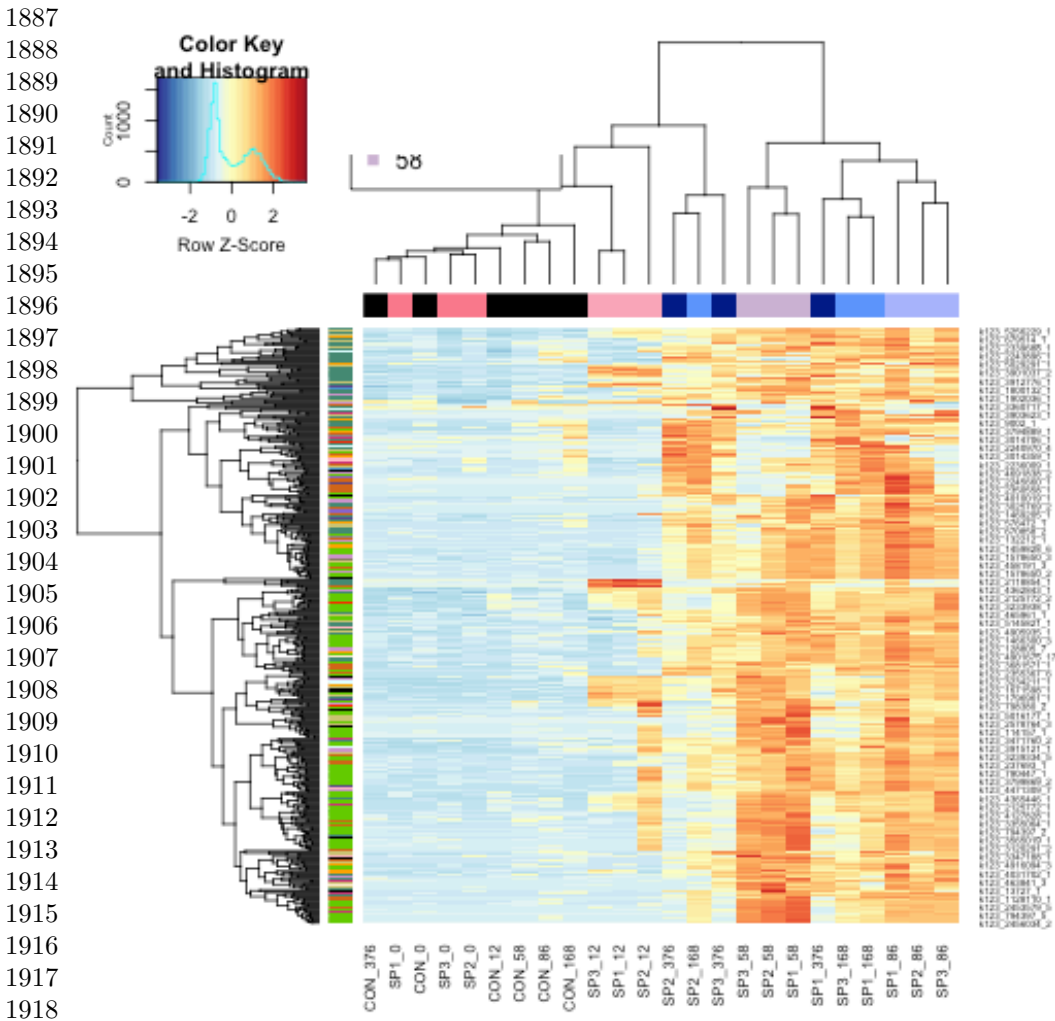
1839

1840





Supplementary Material 1: Figure S1. Soil physiochemical parameters in decomposition soils during the one-year study. Data is shown for each individual donor: SP1 (gold), SP2 (blue), and SP2 (black). Values for the full 16 cm core samples were estimated by summing values interface (0-1 cm) and core (0-16 cm) reported by Taylor et al, (2024) in 1:16 and 15:16 ratios, respectively. Controls reported here are means of three experimental controls that were unimpacted by decomposition and are represented by stars.



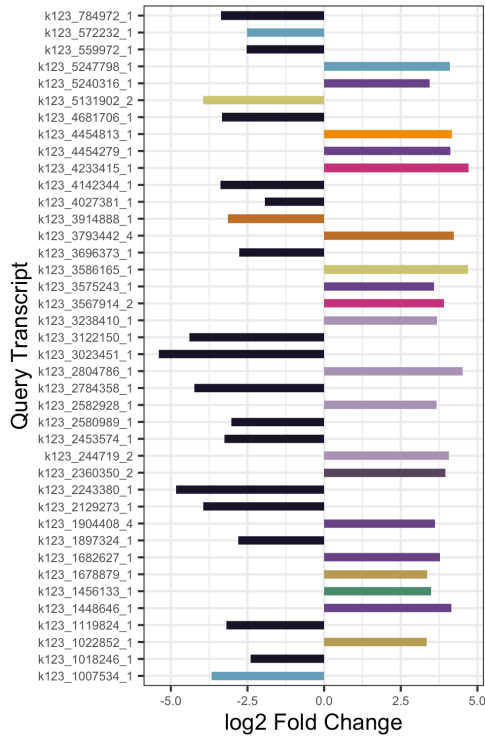
Supplementary Material 2: Figure S2. Hierarchical clustering heatmap showing the log counts per million (CPM) of the top 500 most variable genes across samples. Variable genes were determined by selecting genes with the highest variance in gene expression. Samples are clustered along the x-axis using Euclidean distances between samples and colored by study day.

Table S1. Permutational analysis of variance (PERMANOVA) results identifying significant environmental parameters which explain some of the variation in soil gene expression profiles. Environmental parameter data is from Taylor et al. (2024).

Variables with  $p < 0.05$  are indicated in bold.

Supplementary Material 3

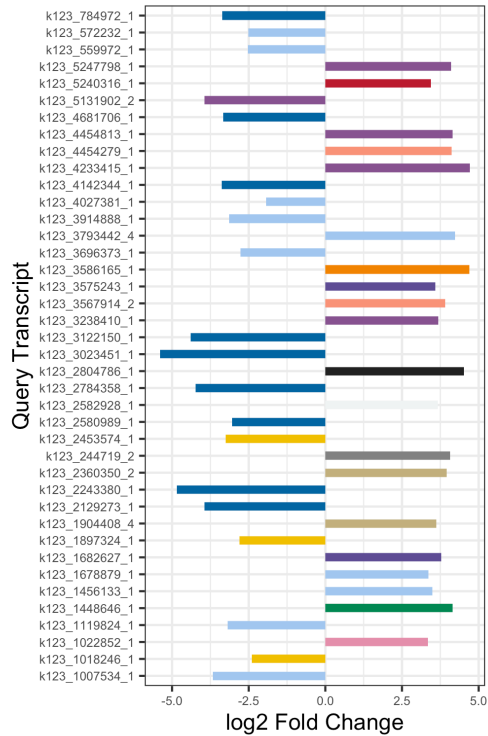
A



## COG Category

- Cell motility
- Energy production and conversion
- Transcription
- Cell cycle control, cell division, chromosome partitioning
- Carbohydrate transport and metabolism
- Intracellular trafficking, secretion and vesicular transport
- Signal transduction mechanisms
- Translation, ribosomal structure and biogenesis
- Post-translational modification, protein turnover, and chaperones
- Function Unknown
- unclassified

B



## Taxonomy

- 1117|Cyanobacteria
- 1236|Gammaproteobacteria
- 135614|Xanthomonadales
- 2|Bacteria
- 200940|Thermodesulfobacteria
- 201174|Actinobacteria
- 203682|Planctomycetes
- 204432|Acidobacteriia
- 2157|Archaea
- 28211|Alphaproteobacteria
- 28221|Deltaproteobacteria
- 4751|Fungi
- 57723|Acidobacteria
- 976|Bacteroidetes

Supplementary Material 4: Figure S3. Top 40 up- and down-regulated genes in controls relative to decomposition soils across all study days, colored by COG functional category (A) and taxonomic annotation (B). Positive values denote higher expression in controls, while negative values are higher in decomposition soils.

1933  
1934  
1935  
1936  
1937  
1938  
1939  
1940  
1941  
1942  
1943  
1944  
1945  
1946  
1947  
1948  
1949  
1950  
1951  
1952  
1953  
1954  
1955  
1956  
1957  
1958  
1959  
1960  
1961  
1962  
1963  
1964  
1965  
1966  
1967  
1968  
1969  
1970  
1971  
1972  
1973  
1974  
1975  
1976  
1977  
1978

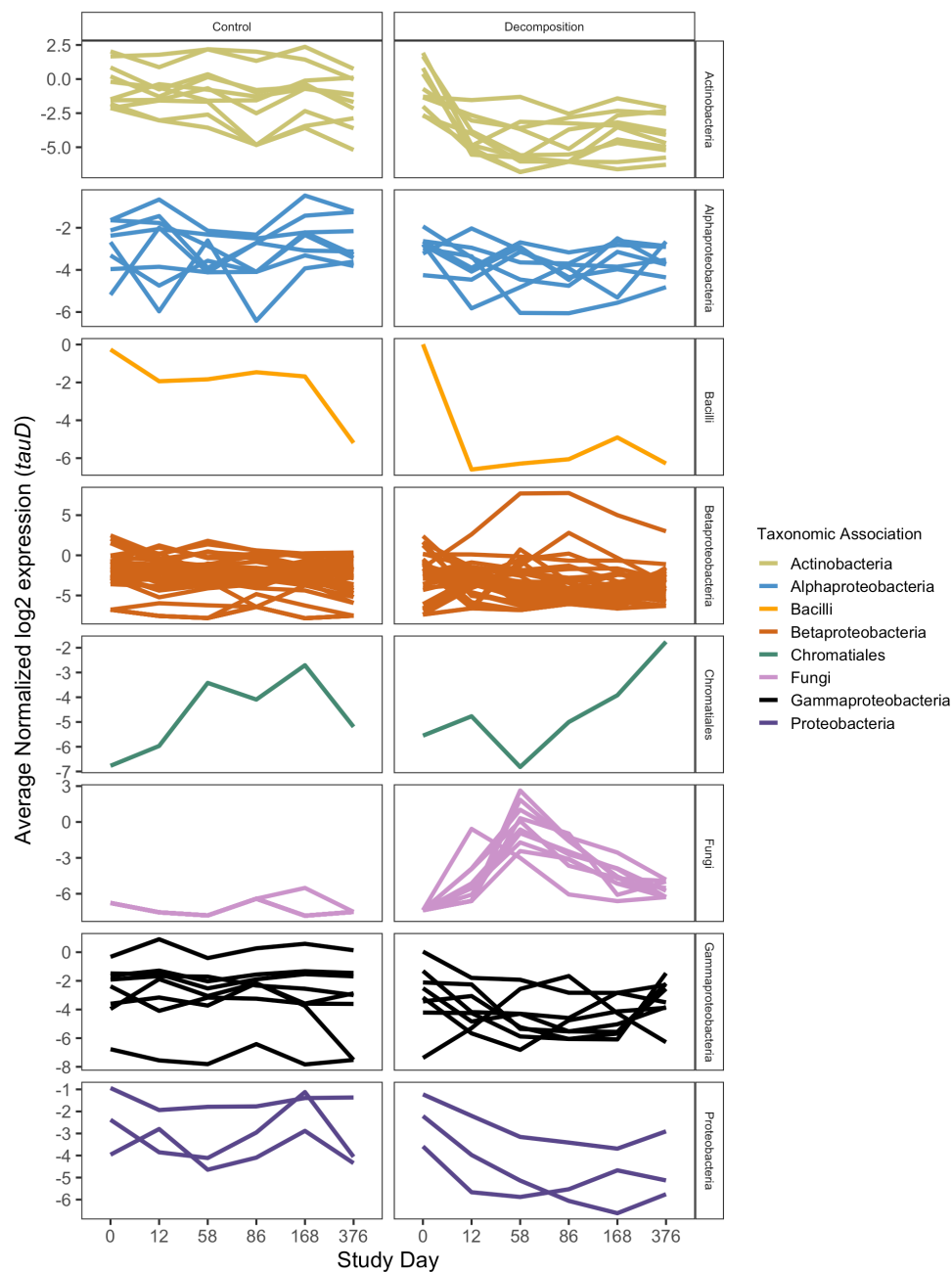
1979  
1980  
1981  
1982  
1983  
1984  
1985  
1986  
1987  
1988  
1989  
1990  
1991  
1992  
1993  
1994  
1995  
1996  
1997  
1998  
1999  
2000  
2001  
2002  
2003  
2004  
2005  
2006  
2007  
2008  
2009  
2010  
2011  
2012  
2013  
2014  
2015  
2016  
2017  
2018  
2019  
2020  
2021  
2022  
2023  
2024

Table S2. Top 20 most up- and down-regulated gene queries, determined by log2 fold change and adjusted p-values, in control relative to decomposition soils. Positive log2 fold change values represent genes whose expression was higher in control soils, while negative log2 fold change values were higher in decomposition soils. Taxonomic annotation, COG categories, gene description, gene names, and EC were assigned via eggNOG-mapper.

Supplementary Material 5

Table S3. Top 10 most up- and down-regulated genes, determined by log2 fold change and adjusted p-values, for each sequential timepoint comparison. Positive log2 fold change values represent genes whose expression was higher in the later decomposition timepoint soils, while negative log2 fold change values are higher in earlier decomposition timepoint soils. Taxonomic annotation, COG categories, gene names, and EC were assigned via eggNOG-mapper. The comparison column distinguishes each timepoint comparison.

Supplementary Material 6



Supplementary Material 7: Figure S4. Mean normalized log<sub>2</sub> expression of *tauD* genes by taxonomic association (color) in control and decomposition soils at each study day. Each line represents one *tauD* gene query, while color denotes taxonomic association as determined by eggNOG-mapper.